Journal of Innate Immunity

Research Article

J Innate Immun 2023;15:614–628
DOI: 10.1159/000530966

Received: November 22, 2022
Accepted: April 13, 2023
Published online: June 29, 2023

Pro-Inflammatory of PRDM1/SIRT2/NLRP3 Axis in Monosodium Urate-Induced Acute Gouty Arthritis

Qingsong Zhao Nan Xia Jinmei Xu Yingnan Wang Luwen Feng
Dihan Su Zhifeng Cheng

Department of Endocrinology, The Fourth Affiliated Hospital of Harbin Medical University, Harbin, PR China

Keywords
Acute gouty arthritis · PR domain-containing 1 with zinc finger domain · Sirtuin 2 · Acetylated α-tubulin · NLR family · Pyrin domain-containing 3 · Macrophages · Inflammatory cytokines

Abstract
PR domain-containing 1 with zinc finger domain (PRDM1) has been reported as a promoter of inflammation, which is a critical process involved in the pathogenesis of acute gouty arthritis. Herein, we sought to ascertain the function of PRDM1 in the development of acute gouty arthritis and related mechanisms. At first, peripheral blood-derived monocytes from patients with acute gouty arthritis and healthy individuals were collected as experimental samples. Then, macrophages were induced from monocytes using phorbol myristate acetate (PMA). The expression patterns of PRDM1, sirtuin 2 (SIRT2), and NLR family, pyrin domain-containing 3 (NLRP3) were characterized by RT-qPCR and Western blot assay. PMA-induced macrophages were stimulated by monosodium urate (MSU) for in vitro experimentation. Meanwhile, a murine model of MSU-induced acute gouty arthritis was established for in vivo validation. PRDM1 was highly expressed while SIRT2 poorly expressed in patients with acute gouty arthritis. Loss of PRDM1 could reduce NLRP3 inflammasome and mature IL-1β levels and downregulate inflammatory cytokines in macrophages, which contributed to protection against acute gouty arthritis. Furthermore, results showed that PRDM1 could inhibit SIRT2 expression via binding to the deacetylase SIRT2 promoter. Finally, the in vivo experiments demonstrated that PRDM1 increased NLRP3 inflammasome and mature IL-1β through transcriptional inhibition of SIRT2, whereby aggravating MSU-induced acute gouty arthritis. To sum up, PRDM1 increased NLRP3 inflammasome through inhibiting SIRT2, consequently aggravating MSU-induced acute gouty arthritis.

Introduction

Gout, prevalent inflammatory arthritis, imposes a heavy and increasing burden on human health owing to the deposition of monosodium urate (MSU) crystals, which are often misdiagnosed and mismanaged [1, 2]. The deposited MSU crystals can lead to inflammatory reactions in human macrophages, which are important links in the pathogenesis of acute gouty [3]. Gout flares require MSU to induce NLRP3 inflammasome activation and sufficient interleukin-1β (IL-1β) secretion [4]. Studies

Qingsong Zhao and Nan Xia are regarded as co-first authors.

karger@karger.com
www.karger.com/jin

Correspondence to:
Zhifeng Cheng, 002537@hrbmu.edu.cn

have highlighted the roles of pro-inflammatory cytokines (IL-1, IL-6, IL-1β, etc.) in the pathogenesis of acute gouty flares, especially NLRP3 inflammasome activation [5, 6], and recent development of several IL-1 inhibitors (anakinra, canakinumab, rilonacept, etc.) provide evidence for their potential roles in the inflammatory process of gout [7, 8]. Due to their high cost and limited clinical experience, it is urgently necessary to seek new targets.

To identify the candidate genes that participate in the pathophysiology of acute gouty arthritis, we conducted an analysis of differential gene expression on a publicly available dataset GSE65931 and identified PR domain-containing 1 with zinc finger domain (PRDM1, the gene encoding Blimp-1) as a gene involved in the development of acute gouty arthritis. Intriguingly, increasing PRDM1 expression induces inflammatory gene expression, and PRDM1 is essential for maintaining the homeostasis of dendritic cells derived from human monocytes [9, 10]. Furthermore, PRDM1 exerts a critical role in the adaptive immune system, especially in the regulation of inflammatory mediators in macrophages and dendritic cells [11]. Thus, we considered that PMDR1 might be a gene associated with the pathogenesis of acute gouty arthritis and hypothesized that PRDM1 may lead to an inflammatory response by stimulating the production of the inflammatory cytokines in acute gouty arthritis.

MSU crystals could also promote cytokine production via activating NLPR3 inflammasome [12], implying the association between NLPR3 and inflammation in acute gouty arthritis. NLR proteins are intracellular regulators of host defense and immunity, and NLRP12 has emerged as a vital regulator for inflammatory gene expression in myeloid cells [13]. Similarly, when MSU crystals are phagocytosed by macrophages, activation of NLRP3 inflammasome and up-regulation of IL-1β contribute to the initiation of acute gouty arthritis [1, 10]. Also, MSU crystals elicit the assembly of NLRP3 inflammasomes to activate caspase-1, leading to the secretion of active IL-1β and IL-18 [14, 15].

Additionally, it has been shown that the knockdown of sirtuin 2 (SIRT2) makes it easier to induce inflammatory responses in mice [16], indicating that SIRT2 could also affect the development of inflammatory responses. SIRT2 is recognized as a nicotinamide adenine dinucleotide (NAD^+)-dependent enzyme that mediates the acetylation of α-tubulin [17]. As previously reported, acetylated α-tubulin mediates dynein-dependent mitochondrial transport and ASC binding to NLRP3 on mitochondria [18]. Hence, SIRT2 may participate in the possible mechanism by which MSU activates NLRP3 inflammasome. To confirm whether there is a correlation between PRDM1, SIRT2, and NLRP3 in macrophages under the induction of MSU crystals, we conducted a series of experiments, hoping to reveal a new mechanism involved in the pathogenesis of MSU-evoked acute gouty arthritis.

Materials and Methods

Ethics Statement

All research protocols were approved by the Clinical Research Ethics Committee and Animal Ethics Committee of the Fourth Affiliated Hospital of Harbin Medical University (2016-393-2) and in keeping with the Declaration of Helsinki for human beings and NIH guidelines for animals. Written informed consent was obtained from patients and for the participants aged under 18, written informed consent was obtained from their legal guardians.

Bioinformatics Analysis

Through the Gene Expression Omnibus (GEO) database, the mRNA expression microarray GSE65931 was downloaded, which contains three MSU-treated cell lines and three normal cells. Through differential analysis of the microarray dataset ($|logFC| > 1$, $p < 0.05$) using the R language "limma" package, MSU-induced differentially expressed genes (DEGs) were selected. From the Human TFs website, a list of transcription factors was obtained followed by prediction of their binding site using the JASPAR database.

Sample Collection

Peripheral blood samples were collected from patients with acute gouty arthritis ($n = 20$) who were diagnosed in the Department of Rheumatology and Immunology of the Fourth Affiliated Hospital of Harbin Medical University from January 2017 to June 2019. All patients received treatments in our hospital, and all peripheral blood samples were collected before treatment. The classification of acute gouty arthritis met the preliminary criteria issued by the American College of Rheumatology on classifying acute arthritis of primary gout [19]. Moreover, healthy participants ($n = 34$) without hyperuricemia, other metabolic syndromes, or chronic diseases were included and their peripheral blood samples were collected. The clinical basic information of acute gouty arthritis patients and healthy participants is detailed in online supplementary Table 1 (for all online suppl. material, see https://doi.org/10.1159/000530966).

Isolation of PBMCs

At first, 30 mL of peripheral blood samples were gained from acute gouty arthritis patients and healthy volunteers. The Ficoll-Paque-PLUS kit (GE Healthcare, Piscataway, NJ, USA) was then used to isolate peripheral blood mononuclear cells (PBMCs). Subsequently, monocytes were isolated from PBMCs using the Human Monocyte Isolation Kit (Miltenyi Biotec, Auburn, CA, USA). The collected cells for enzyme-linked immunosorbent assay (ELISA) assay were stored at −80°C.

Cell Culture and Transfection

The human monocyte cell line THP-1 (supplied by Shanghai Cell Bank, Chinese Academy of Sciences, Shanghai, China) was selected and cultured in RPMI-1640 medium (22400089, Invitrogen, USA)

that contained 10% fetal bovine serum (FBS, 100099141, Gibco, Carlsbad, CA, USA), 1% penicillin-streptomycin (15070063, Gibco), and 2 mmol/L glutamine (25030081, Gibco). The culture of 293T cells (Wuhan Procell Life Science & Technology Co., Ltd., Hubei, China) was proceeded in Dulbecco's Modified Eagle Medium (DMEM) (10569044, Gibco) that encompassed 10% FBS (10099141), 1% penicillin-streptomycin (15070063), and 1% glutamine (25030081). All cells were cultured at 37°C with 5% CO_2, detached with 0.25% trypsin, and then passaged at a ratio of 1: 3. To obtain macrophages, log-phase THP-1 cells were induced with 50 ng/mL of phorbol myristate acetate (PMA, 10 mg/mL, 16561-29-8, Solarbio) for 48 h prior to the in vitro experiments.

Core plasmid (pLKO.1) and helper plasmid (psPAX2, pMD2.G) of the silencing sequence of the target genes as well as core plasmid (pHAGE-CMV-MCS-IzsGreen) and helper plasmid (psPAX2, pMD2.G) of the cDNA sequence of the target genes were employed to package silencing and overexpression lentiviruses, respectively. All lentiviruses were supplied by Shanghai Sangon Biotechnology Co., Ltd. (Shanghai, China), and primer sequencing and plasmid construction were also implemented by Sangon.

The packaging lentiviruses and target vectors were co-introduced into 293T cells as per the specifications of Lipo2000 kit (11668-019, Invitrogen). The supernatant was collected 48 h after cell culture, which contained viral particles after filtering and centrifugation. Following detection of virus titer, lentiviruses carrying shRNA (sh)-negative control (NC), oe-NC, sh-PRDM1-1, sh-PRDM1-2, sh-SIRT2-1, sh-SIRT2-2, or oe-PRDM were maintained for use. When the cell growth was in the logarithmic phase, the cells were trypsinized, prepared into cell suspension (5×10^4 cells/mL), and seeded in a 6-well plate (2 mL in each well), followed by culture at 37°C overnight. At 48 h post-infection, the relevant genes in the lentivirus-treated cells were assayed by reverse transcription-quantitative polymerase chain reaction (RT-qPCR). The shRNA sequences for PRDM1 and SIRT2 are shown in online supplementary Table 2. The lentivirus-infected cell line was screened as a stable cell line.

MSU-Induced Acute Gouty Arthritis Model in vitro

A total of 4×10^5 PMA-induced cells (macrophages) were seeded in 12-well plates and incubated overnight. Opti-MEM (31985070, Sigma-Aldrich, St Louis MO, USA) was added for subsequent culture. Cells were stimulated with MSU (50 μg/mL, 100 μg/mL, InvivoGen, CA, USA) for 18 h. Culture supernatants were collected for cytokine analysis by ELISA, or RNA was extracted for RT-qPCR analysis.

RT-qPCR

Total RNA was extracted from cells with Trizol (16096020, Thermo Fisher Scientific, Rockford, IL, USA), and mRNA was reversely transcribed into complementary DNA (cDNA) as per protocols of the first-strand cDNA synthesis kit (D7168L; Beyotime, Shanghai, China). RT-qPCR experiments were performed as per the instructions of the RT-qPCR kit (Q511-02; VazymeBiotech, Nanjing, Jiangsu, China). Briefly, 2 μL of cDNA template, 0.2 μL of upstream primer, 0.2 μL of downstream primer, and 10 μL of RT-qPCR Mix were mixed and supplemented to 20 μL with RNAase-free water. A Bio-rad real-time qPCR instrument CFX96 (BIO-RAD, Hercules, CA, USA) was adopted for PCR amplification under the reaction conditions: pre-denaturation at 95°C for 30 s, and a total of 40 cycles of denaturation at 95°C for 10 s, annealing at 60°C for 30 s, and extension at 72°C for 30 s, with a dissolution curve of 65°C–95°C. Primer sequences were designed and supplied by Sangon, as listed in online supplementary Tables 3 and 4. Fold alterations in expression relative to the loading control β-actin were calculated by the $2^{-\Delta\Delta Ct}$ method.

Western Blot Assay

Radio immunoprecipitation assay (RIPA) lysis buffer containing PMSF (P0013B, Beyotime) was added to lyse tissues and cells to extract total protein according to instructions of the kit (P0028, Beyotime). Protein concentration in the supernatant of each sample was assayed with a bicinchoninic acid kit (P0011, Beyotime), and adjusted to 1 μg/μL. For electrophoretic separation, 8–12% sodium dodecyl sulfate gels were prepared, and protein samples were added equally to each lane with a micropipette. The proteins on the gels were placed onto a PVDF membrane (1620177; BIO-RAD), which was blocked with 5% skimmed milk or 5% bovine serum albumin for 1 h. After that, rabbit anti-β-actin (4970, 1:5,000, Cell Signaling Technologies [CST], Beverly, MA, USA), rabbit anti-PRDM1 (9115, 1:1,000, CST), rabbit anti-cleaved caspase-1 (4199, 1:1,000, CST), rabbit anti-pro-IL-1β (12703, 1:1,000, CST), rabbit anti-cleaved IL-1β (83186, 1:1,000, CST), rabbit anti-SIRT2 (12672, 1:1,000, CST), rabbit anti-procaspase-1 (3866, 1:1,000, CST), rabbit anti-NLRP3 (15101, 1:1,000, CST), rabbit anti-ASC (67824, 1:1,000, CST), rabbit anti-AC-α-tubulin (5,335, 1:5,000, CST), mouse anti-α-tubulin (3873, 1:5,000, CST), and rabbit anti-histone deacetylase 6 (HDAC6; 7558, 1:1,000, CST) were loaded on the membrane for incubation overnight at 4°C. Following three washes with 1 × Tris Buffered Saline Tween for 5 min, incubation together with HRP-labeled secondary antibody of goat anti-rabbit or mouse immunoglobulin G (IgG; ab6721 or ab205719, 1:5,000; Abcam, Cambridge, UK) lasted for 1 h. After washes, the membrane was immersed in enhanced chemiluminescence solution (1705062; BIO-RAD) for 1 min. Images were captured by an ImageQuantLAS4000C gel imager (GE Company, Schenectady, NY, USA). The gray values of the target bands normalized to internal control β-actin were used as the relative expression of the proteins.

ELISA

The levels of IL-1β (SLB50; Biotech, USA), IL-6 (S6050, Biotech, Texas, Huston, USA), IL-18 (DY318-05, Biotech), and TNF-α (210-TA-005, Biotech) in clinical peripheral blood samples and cell supernatant, as well as IL-1β (SMLB00C, Biotech), IL-6 (SM6000B, Biotech), IL-18 (DY122-05, Biotech), and TNF-α (SMTA00B, Biotech) levels in RIPA homogenate supernatant of mouse foot tissues, were measured following the instructions of the ELISA kit.

Immunofluorescent Staining

A total of 1×10^6 cells were seeded on confocal culture dishes. The cells reaching 60% confluence were fixed in 95% absolute ethanol for 15 min, washed with cold PBS, and then incubated with 5% bovine serum albumin, followed by incubation with specific rabbit anti-NLRP3 (ab4207, 1:200; Abcam), rabbit anti-ASC (67824, 1:800, CST), rabbit anti-AC-α-tubulin (5,335, 1:800, CST), and mouse anti-α-tubulin (3873, 1:2000, CST) overnight at 4°C. Fluorescent goat anti-mouse or rabbit IgG H&L (ab6785 or

ab6717, 1:100; Abcam) was selected as secondary antibody for 2-h incubation at 37°C. Then, the cells were co-incubated with DAPI for 15 min at ambient temperature. Lastly, staining images were captured for observation under a confocal scanning microscope (LSM700; CarlZeiss, Oberkochen, Germany).

NAD^+ Measurement

Nicotinamide adenine dinucleotide (NAD^+/NADH) was quantified in the treated macrophages according to the kit (MAK037, Sigma-Aldrich) instructions. Briefly, samples were extracted from cells or tissues with buffer solution and deproteinized with a spin column. Then, samples and standards were delivered to the wells, which were reacted with mixture for 5 min to convert NAD to NADH. Afterward, NADH developer was added for 1–4 h of incubation while reaction cycles, during which the analysis was performed several times using a microplate reader. The reaction can be stopped with a stop solution.

Dual Luciferase Reporter Gene Assay

SIRT2 dual-luciferase reporter gene vectors and mutant plasmids (site1-3 deletion) with mutated PRDM1 binding sites, PGL3-basic-SIRT2-WT and PGL3-basic-SIRT2-MUT, were constructed, respectively. The reporter plasmid oe-PRDM1 and NC plasmids were co-transfected into 293T cells, respectively. 24 h later, the cells were lysed and centrifuged at 10,000 *g* for 1 min. Luciferase activity in the supernatant was then measured using the Dual-Luciferase® Reporter Assay System (E1910; Promega, Madison, WI, USA). The Firefly/Renilla luciferase activity ratio was calculated.

Chromatin Immunoprecipitation Assay

Chromatin immunoprecipitation (ChIP) assay was conducted using the ChIP kit SimpleChIP® Enzymatic Chromatin IP Kit (Magnetic Beads) (9003, CST). Briefly, about 3×10^7 cells reaching 95% confluence were cross-linked by incubation with 1% formaldehyde for 10 min at room temperature, which was stopped by the addition of glycine solution. Cells were washed twice with cold PBS and added to cold PBS containing protease inhibitors. Nuclear lysates were sonicated 15 times for 10 s, yielding DNA fragments between 200 and 300 bp in size. The sheared chromatin lysate was incubated with 5 μg of histone antibody, 5 μg of PRDM1 antibody (9115, 1:200, CST), and 5 μg of normal IgG overnight at 4°C. Using 30 μL of protein G beads, the harvested immunoprecipitates were eluted three times with low-salt washing buffer, once with high-salt washing buffer, and suspended in elution buffer. Subsequently, reverse cross-linking was performed by incubation with 6 μL of 5 M NaCl and 2 μL of proteinase K at 65°C for 2 h. Finally, the samples were subjected to DNA purification with purification columns. The extracted DNA and SIRT2 primers (sequences shown in online suppl. Table 5) were used for qPCR detection.

Construction of MSU-Induced Acute Gouty Arthritis Mouse Models

C57BL/6 mice (7–8 weeks of age) were administered with 50 μL adenovirus (Ad) (5×10^{11} TU/mL) in the sole of the right paw. 48 h later, MSU crystals (2 mg dissolved in sterile, endotoxin-free PBS) or PBS were injected into the sole of the right paw of mice. Mice were randomly injected with PBS, MSU, PRDM1 siRNA, or SIRT2 siRNA, respectively (the number of mice in each group was 12). The thickness of mouse footpads was observed at 0, 6, 12, and 24 h after injection of MSU crystals, and 24 h later, the foot tissue was homogenized by RIPA buffer, and the attained supernatant was preserved for Western blot and ELISA assays. Additionally, Ad-si-PRDM1 (5′-GTTTACGCAATTCTCGAGAAT-3′), Ad-Con-siRNA (5′-CCTAAGGTTAAGTCGCCCTCG-3′), and Ad-si-SIRT2 (5′-GAGAAGTACCTCGAGGTACTT-3′) were supplied by Shanghai Geneland Biotech Co., Ltd. (Shanghai, China).

Immunohistochemistry

Sagittal sections of the footpads of the acute gouty arthritis mouse models were prepared. Following antigen retrieval and normal goat serum blocking (Sangon), the sections were probed overnight in a dark room with rabbit anti-caspase-1 (ab138483, 1:100; Abcam) and mouse anti-IL-1β (12242, 1:100, CST). Next day, the sections were re-probed with secondary goat anti-rabbit or mouse IgG, followed by incubation with SABC (Vector, Burlingame, CA, USA) for 30 min in a 37°C incubator. After using the DAB Kit (P0203, Beyotime) for color development for 6 min, the sections were dyed utilizing hematoxylin for 30 s. Before observation, the sections were conventionally treated and finally immersed with neutral resin. At last, the sections were observed under a positive microscope (BX63, Japan) for three times. PBS instead of primary antibody was adopted as a negative control. Immunohistochemistry (IHC) images of five different fields were selected for quantitative analysis, and the number of cells with brown-stained signal in the cytoplasm (positively stained cells) and the number of total cells were counted to calculate the proportion of positive cells. The proportion of positive cells = the number of brown-stained cells/the number of total cells × 100%.

Statistical Analysis

All data in this study were analyzed using SPSS 21.0 (IBM, Armonk, NY, USA) software. Measurement data were expressed as mean ± standard deviation. Unpaired *t* test was adopted for data comparisons between two groups, while one-way analysis of variance (ANOVA) followed by Tukey's post hoc test was employed for multiple group comparisons. Repeated measures ANOVA and Tukey's post hoc test were used for time-based data comparisons. A value of $p < 0.05$ was interpreted to denote statistically significant difference.

Results

PRDM1 Promotes the Release of Inflammatory Cytokines from MSU-Induced Macrophages

Through bioinformatics analysis based on the GSE65931 dataset, 108 DEGs were screened (online suppl. Fig. 1a, b). Since transcription factors play a key role in regulating biological processes, we obtained a list of transcription factors from the Human TFs website and intersected them with the DEGs of the GSE65931 dataset to obtain seven MSU-induced differentially expressed transcription factors (online suppl. Fig. 1c). We identified changes in the 7 transcription factor expression in MSU-induced macrophages by RT-qPCR and found most significantly upregulated PRDM1 expression (Fig. 1a). Thus, we predicted that PRDM1 may contribute to acute gouty arthritis.

To test the hypothesis, we used RT-qPCR to detect PRDM1 expression in PBMCs of acute gouty arthritis samples and healthy samples, and the results presented a markedly higher PRDM1 expression in acute gouty arthritis samples than in healthy samples (Fig. 1b). ELISA detection results further exhibited that pro-inflammatory proteins IL-1β, IL-18, TNF-α, and IL-6 in acute gouty arthritis samples were noticeably higher than those in healthy samples (Fig. 1c). Next, PRDM1 expression remarkably increased at a protein level with the increase in MSU concentration (Fig. 1d), and ELISA results revealed that the contents of the aforementioned pro-inflammatory markers in the supernatant of macrophages were notably raised with the increase in MSU concentration (Fig. 1e). Afterward, MSU at a concentration of 100 μg/mL [20] was used in our experiments.

To further examine the relationship between PRDM1 and the release of inflammatory cytokines by macrophages, we constructed macrophages with silenced PRDM1, and Western blot and RT-qPCR data (Fig. 1f) revealed that both sh-PRDM1-1 and sh-PRDM-2 reduced PRDM1 expression, and sh-PRDM1-1 with more significant silencing efficiency was used for subsequent experiments. Furthermore, ELISA results showed that silencing of PRDM1 reduced the contents of the pro-inflammatory cytokines in the MSU-treated macrophages (Fig. 1g).

Subsequently, we constructed a stable cell line overexpressing PRDM1 (PMDR1-macrophages), and Western blot and RT-qPCR analyses of its overexpression efficiency revealed that PRDM1 protein expression and mRNA levels were significantly increased in PMDR1-macrophages (Fig. 1h, i). Western blot results demonstrated that the expression of PRDM1 protein was significantly increased after PRDM1 overexpression in MSU-treated macrophages (Fig. 1j). ELISA results unraveled that the contents of the pro-inflammatory markers were notably increased in PMDR1-macrophages with or without MSU treatment (Fig. 1k). Taken together, PRDM1 may promote the release of inflammatory cytokines from MSU-induced macrophages, thereby deteriorating acute gouty arthritis.

PRDM1 Increases NLRP3 Inflammasome and Mature IL-1β Levels

Existing literature has reported that upon phagocytosis of MSU crystals by macrophages, NLRP3 inflammasome could be activated by the Toll-like receptors such as TLR2 and TLR4 to produce IL-1β, which is cleaved by active caspase-1 to form mature IL-1β [21], thus eliciting a strong inflammatory response in patients with acute gouty arthritis. To investigate the mechanism by which PRDM1 promotes the release of inflammatory cytokines from macrophages to induce acute gouty arthritis, we first speculated whether PRDMI could increase the NLRP3 inflammasome levels to facilitate the release of inflammatory cytokines.

Through NLRP3 expression determination in acute gouty arthritis samples and healthy samples using RT-qPCR, the mRNA level of NLRP3 in acute gouty arthritis samples was determined to be noticeably higher than that in healthy samples (Fig. 2a). We then measured the expression of cleaved caspase-1, pro-caspase-1, cleaved IL-1β, pro-IL-1β, and NLRP3 in the macrophages treated with MSU- or sh-PRDM1 using Western blot analysis, and found that MSU induced markedly enhanced cleaved caspase-1, cleaved IL-1β, and NLRP3 protein levels, which was reversed by knockdown of PRDM1, while that of pro-caspase-1 and pro-IL-1β remained unaffected after the above treatments (Fig. 2b). Subsequently, the macrophages were treated with oe-PRDM1 or MSU. The oe-PRDM1 treatment increased cleaved caspase-1, cleaved IL-1β, and NLRP3 expression in the macrophages with or without MSU treatment; whereas, that of pro-caspase-1 and pro-IL-1β also remained unaltered after the above treatments (Fig. 2c). Altogether, PRDM1 could increase NLRP3 inflammasome and mature IL-1β to enhance the release of IL-1β, TNF-α, IL-6, and IL-18 inflammatory cytokines.

PRDM1 Promotes the Accumulation of α-tubulin Acetylation

To further understand how PRDM1 modulates NLRP3 inflammasome, we first measured the α-tubulin acetylation levels in 20 acute gouty arthritis samples and 34 healthy samples, and the results displayed a significant increase α-tubulin acetylation expression in acute gouty arthritis samples versus healthy samples (Fig. 3a). Western blot results further revealed a consistent increase in the acetylated α-tubulin expression in the MSU-treated cells, which was counteracted by sh-PRDM1 treatment; no marked differences concerning α-tubulin expression were detected after the above treatments (Fig. 3b). Besides, acetylated α-tubulin expression was considerably rescued after oe-PRDM1 treatment or after MSU treatment and was enhanced after co-treatment with oe-PRDM1 and MSU; however, α-tubulin expression exhibited no noticeable alteration after the above treatments (Fig. 3c). These results supported that MSU treatment or overexpression of PRDM1 could lead to increased α-tubulin acetylation.

In attempt to further substantiate the promotive role of PRDM1 in α-tubulin acetylation, α-tubulin, and acetylated α-tubulin levels in cells were assayed by immunofluorescence,

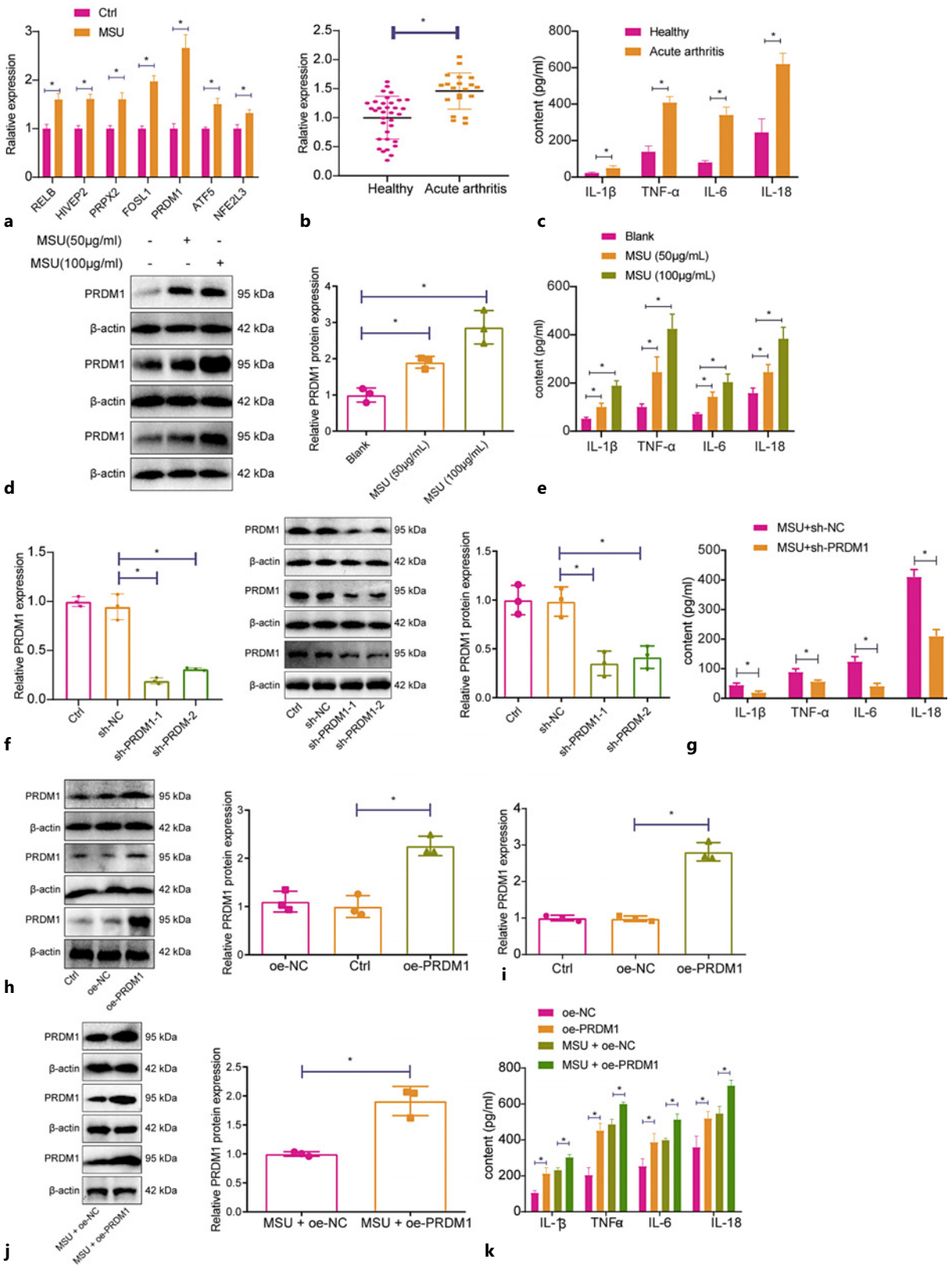

1

(For legend see next page.)

respectively. As outlined in Fig. 3d, e, the treatment of MSU significantly increased acetylated α-tubulin, which was offset by the additional treatment of sh-PRDM1. Overexpression of PRDM1 increased acetylated α-tubulin with or without MSU treatment in cells. Because of the increase in acetylated α-tubulin, we examined the expression of two deacetylases, SIRT2 and HDAC6, and found that SIRT2 expression was considerably repressed by MSU treatment, which was counteracted by sh-PRDM1 treatment (Fig. 3f). SIRT2 was notably downregulated after oe-PRDM1 treatment, while the SIRT2 expression was further decreased after additional treatment of MSU (Fig. 3g). Additionally, there were no significant changes in HDAC6 expression after these treatments. Taken together, knockdown of SIRT2 expression by PRDM1 promoted acetylated α-tubulin accumulation in cells, thereby increasing NLRP3 inflammasome levels.

PRDM1 Binds to the SIRT2 Promoter to Repress Its Transcription

Next, we further interrogated the relationship between PRDM1 and SIRT2. First, RT-qPCR results presented a significant deficiency in SIRT2 expression in acute gouty arthritis samples as compared to healthy samples (Fig. 4a). SIRT2 is an NAD^+-dependent enzyme, and NAD^+ level plays an important role in SIRT2 activity [17]. Hence, we speculated that PRDM1 might inhibit SIRT2 expression by inhibiting intracellular NAD^+ level. First, the results confirmed no significant difference in NAD^+ levels after overexpression or inhibition of PRDM1 (Fig. 4b). This indicated that inhibition of SIRT2 expression by PRDM1 might directly regulate the SIRT2 expression but not through regulation of the intracellular NAD^+ level. Through JASPAR database analysis, PRDM1 binding sites were found in the SIRT2 promoter region (Fig. 4c). Luciferase assay results offered evidence that PRDM1 could bind to the SIRT2 promoter and inhibit its transcriptional activity (Fig. 4d, e), and ChIP assay results validated that MSU crystal stimulation strengthened the binding of PRDM1 to the SIRT2 promoter region (Fig. 4f). These results indicated that PRDM1 bound to the SIRT2 promoter to inhibit SIRT2 transcription, thereby inhibiting SIRT2 expression.

PRDM1 Targets SIRT2 and Increases NLRP3 Inflammasome and Mature IL-1β to Facilitate the Release of Inflammatory Cytokines from Macrophages in the Context of MSU Stimulation

Previous research has reported that SIRT2 knockdown is able to induce inflammatory responses in mice [16], indicating the importance of SIRT2 in the development of inflammatory responses. Next, we interrogated the relationship between PRDM1/SIRT2 and NLRP3 inflammasome. First, RT-qPCR results displayed better silencing efficiency of sh-SIRT2-1 relative to sh-SIRT2-2, and sh-SIRT2-1 was thus used for the subsequent experiments, whilst the SIRT2 expression was further decreased by SIRT2 knockdown in the presence of sh-PRDM1 (Fig. 5a).

Next, Western blot results revealed that SIRT2 knockdown induced no significant difference regarding PRDM1, pro-caspase-1, and pro-IL-1β expression, a decrease in SIRT2 expression, and an increase in cleaved caspase-1, cleaved IL-1β, and NLRP3 expression after treatment of MSU and sh-PRDM1 (Fig. 5b). ELISA revealed that the contents of pro-inflammatory cytokines were all significantly increased after treatment of sh-SIRT2 in the MSU and sh-PRDM1-treated cells (Fig. 5c). From the above Figure 1d, treatment of MSU and sh-PRDM1 together reduced the release of inflammatory cytokines than MSU alone, but the inflammatory cytokine release was increased again after continued silencing of SIRT2. Altogether, PRDM1 increased NLRP3 inflammasome and mature IL-1β by inhibiting SIRT2 expression, thereby promoting the secretion of inflammatory cytokines from macrophages in the context of MSU stimulation.

Fig. 1. PRDM1 promotes the release of inflammatory cytokines from MSU-induced macrophages. **a** RT-qPCR determination of the expression of 7 transcription factors in the control group and MSU-treated group. **b** RT-qPCR determination of PRDM1 expression in 20 acute gouty arthritis samples and 34 healthy samples. **c** ELISA detection of IL-1β, TNF-α, IL-6, and IL-18 contents. **d** Western blot detection of PRDM1 expression in cells stimulated with MSU crystals. **e** IL-1β, TNF-α, IL-6, and IL-18 contents in the supernatant of cell culture medium after MSU treatment. **f** Relative PRDM1 expression and protein level in PMA-induced macrophages measured by Western blot and RT-qPCR analysis, respectively. **g** ELISA detection of the contents of IL-1β, TNF-α, IL-6, and IL-18 in the supernatant of MSU- or sh-PRDM1-treated cell culture medium. **h** PRDM1 overexpression efficiency in cells detected by Western blot. **i** PRDM1 overexpression efficiency in cells validated by RT-qPCR. **j** PRDM1 expression in cells after MSU + oe-PRDM1 treatment detected by Western blot. **k** ELISA detection of IL-1β, TNF-α, IL-6, and IL-18 contents in the supernatant of MSU- or oe-PRDM1-treated cell culture medium. $^*p < 0.05$.

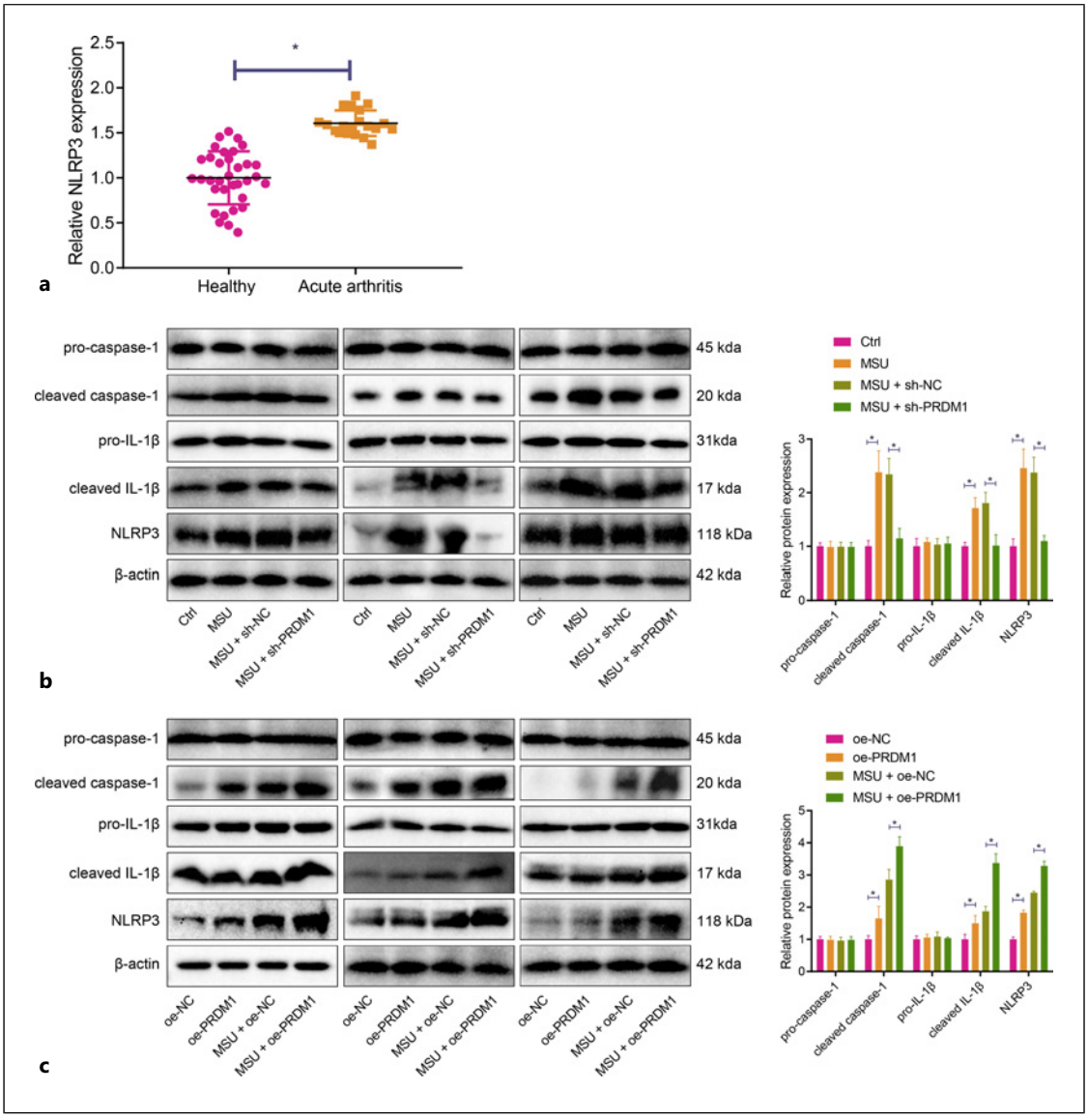

Fig. 2. PRDM1 knockdown decreases NLRP3 inflammasome and mature IL-1β levels and decreases the release of inflammatory cytokines. **a** RT-qPCR determination of NLRP3 expression in 20 acute gouty arthritis samples and 34 healthy samples. **b** Western blot analysis of cleaved caspase-1, pro-caspase-1, cleaved IL-1β, pro-IL-1β, and NLRP3 expression in cells treated with MSU- or sh-PRDM1. **c** Western blot analysis of cleaved caspase-1, pro-caspase-1, cleaved IL-1β, pro-IL-1β, and NLRP3 expression in cells treated with MSU- or oe-PRDM1. *$p < 0.05$.

PRDM1 Induces Acute Gouty Arthritis Flares by Inhibiting SIRT2 Expression and Activating NLRP3 Inflammasome in Mice

To further verify the relationship between PRDM1 and acute gouty arthritis flares, we performed an in vivo experiment in mice. First, we measured the thickness of footpads in mice injected with MSU crystals at 0, 6, 12, and 24 h (Fig. 6a). Correspondingly, MSU crystals notably augmented the footpad thickness of mice, whilst further silencing PRDM1 reduced the footpad thickness of MSU-treated mice, and the role of PRDM1 knockdown on the MSU-treated mice footpad thickness was counteracted by downregulating SIRT2. Western blot and RT-qPCR results displayed that MSU noticeably upregulated PRDM1 and NLRP3 expression while reducing SIRT2 expression in foot tissues of mice, while further depletion of PRDM1 caused opposite trends. In MSU-treated mice with silenced PRDM1, silencing of SIRT2 led to no

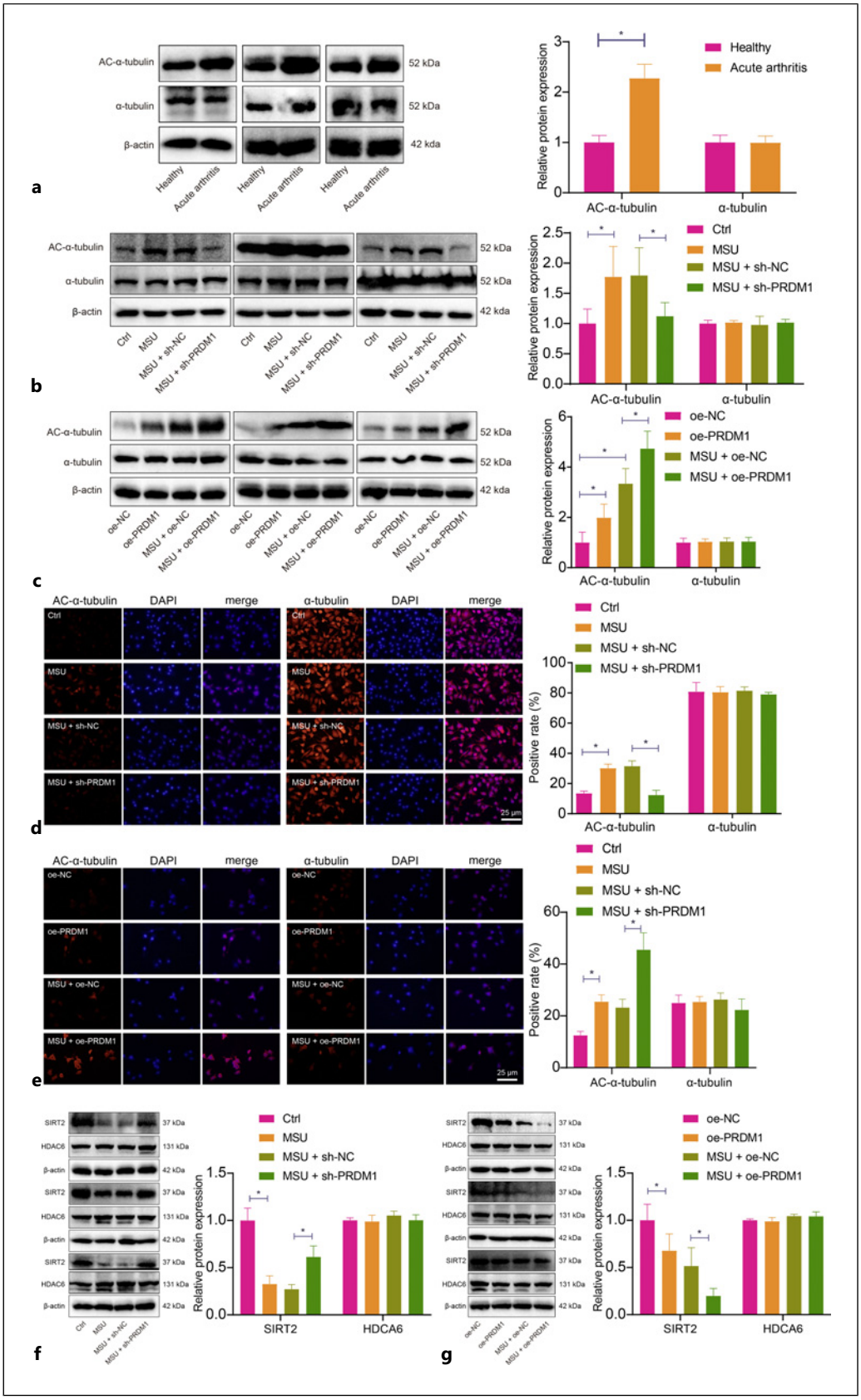

Fig. 3. PRDM1 promotes the accumulation of α-tubulin acetylation by increasing NLRP3 inflammasome in the context of MSU stimulation. **a** Western blot analysis of α-tubulin acetylation levels in 20 acute gouty arthritis samples and 34 healthy samples. **b** Western blot analysis of α-tubulin acetylation levels in cells treated with MSU- or sh-PRDM1. **c** Western blot analysis of α-tubulin acetylation levels in cells treated with MSU- or oe-PRDM1. **d** The expression of α-tubulin and acetylated α-tubulin in cells treated with MSU- or sh-PRDM1 detected by immunofluorescence. **e** The expression of α-tubulin and acetylated α-tubulin in cells treated with MSU- or oe-PRDM1 detected by immunofluorescence. **f** The expression of SIRT2 and HDAC6 in cells treated with MSU- or sh-PRDM1 detected by Western blot. **g** The expression of SIRT2 and HDCA6 in cells treated with MSU- or oe-PRDM1 detected by Western blot. *$p < 0.05$.

J Innate Immun 2023;15:614–628
DOI: 10.1159/000530966

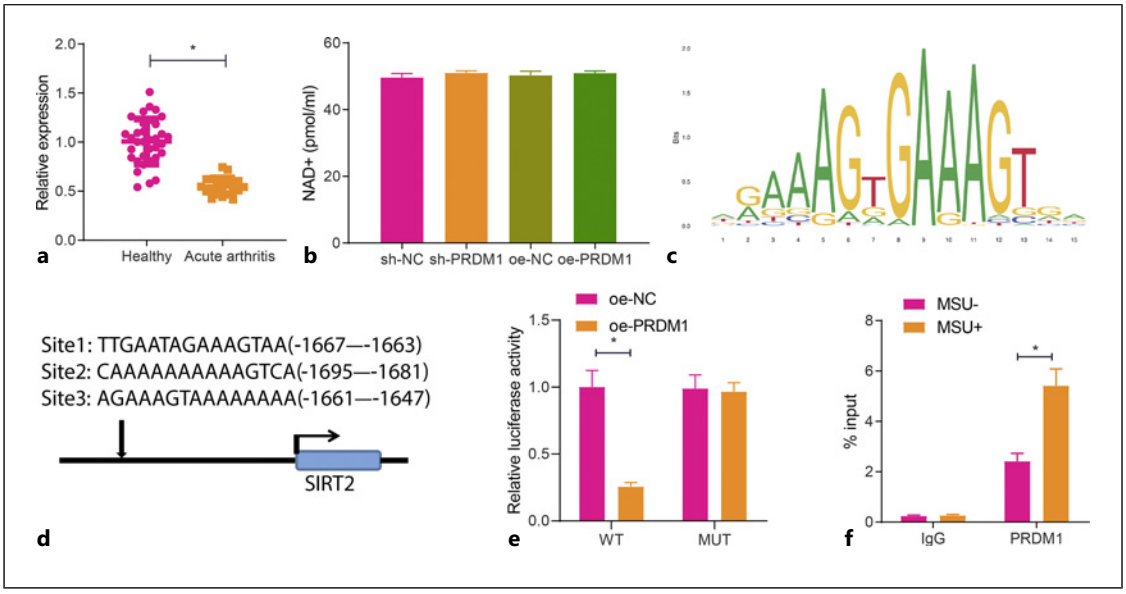

Fig. 4. PRDM1 targets SIRT2. **a** RT-qPCR determination of SIRT2 expression in 20 acute gouty arthritis samples and 34 healthy samples. **b** NAD^+ levels in sh-/oe-PRDM1-treated cell culture medium. **c** Specific binding motifs of PRDM1 on the SIRT2 promoter obtained through JASPAR database analysis. **d** Prediction of binding sites between PRDM1 and SIRT2. **e** The relationship between PRDM1 and SIRT2 verified by dual-luciferase reporter gene assay. **f** The binding of PRDM1 to SIRT2 after MSU crystal stimulation verified by ChIP assay. $^*p < 0.05$.

changes in PRDM1 expression, reduced SIRT2 expression, and increased NLRP3 expression (Fig. 6b, c).

ELISA detection revealed that MSU markedly increased the contents of the inflammation-promoting proteins in mouse foot tissues, which were reversed by silencing of PRDM1. Besides, SIRT2 knockdown increased the contents of the inflammation-promoting protein that were reduced by silencing PRDM1 in the presence of MSU (Fig. 6d). IHC results further supported that MSU increased the expression of caspase-1 and IL-1β in mouse foot tissues, while further silencing of PRDM1 resulted in the opposite trends. Additionally, SIRT2 depletion increased the expression of caspase-1 and IL-1β that was downregulated by knocking down PRDM1 in the presence of MSU (Fig. 6e). The above results indicated that PRDM1 could increase NLRP3 inflammasome as well as inflammatory cytokines released from macrophages by inhibiting SIRT2, aggravating MSU-induced acute gouty arthritis.

Discussion

For the mechanism underlying MSU-evoked acute gouty arthritis, we experimentally confirmed that MSU crystals could result in increased intracellular PRDM1 expression, which targeted the deacetylase SIRT2, resulted in massive accumulation of acetylated α-tubulin and promoted the levels of NLRP3 inflammasome, thereby stimulating macrophages to release large amounts of the inflammatory cytokines and consequently aggravating MSU-induced acute gouty arthritis (Fig. 7).

Initially, we experimentally determined that PRDM1 promoted the secretion of pro-inflammatory cytokines encompassing IL-1β, TNF-α, IL-6, and IL-18 from macrophages to exacerbate MSU-induced acute gouty arthritis. PBMCs from patients with acute gouty arthritis can release larger amount of pro-inflammatory cytokines than those from healthy people [12], indicating that accumulation of pro-inflammatory cytokines is a marker of acute gouty arthritis. Mounting literature has also shown the involvement of IL-1β, IL-8, IL-17, and TNF-α in the MSU-induced inflammatory process such as acute gouty arthritis [2, 21]. Of note, increasing PRDM1 expression has been indicated to stimulate the release of inflammatory markers [10], suggesting the correlation of PRDM1 with pro-inflammatory cytokine production. Consistently, this study determined increased expression of these pro-inflammatory cytokines in MSU-treated macrophages after PRDM1 overexpression. From above, the stimulative role of PRDM1 in the production of inflammatory cytokine is partially

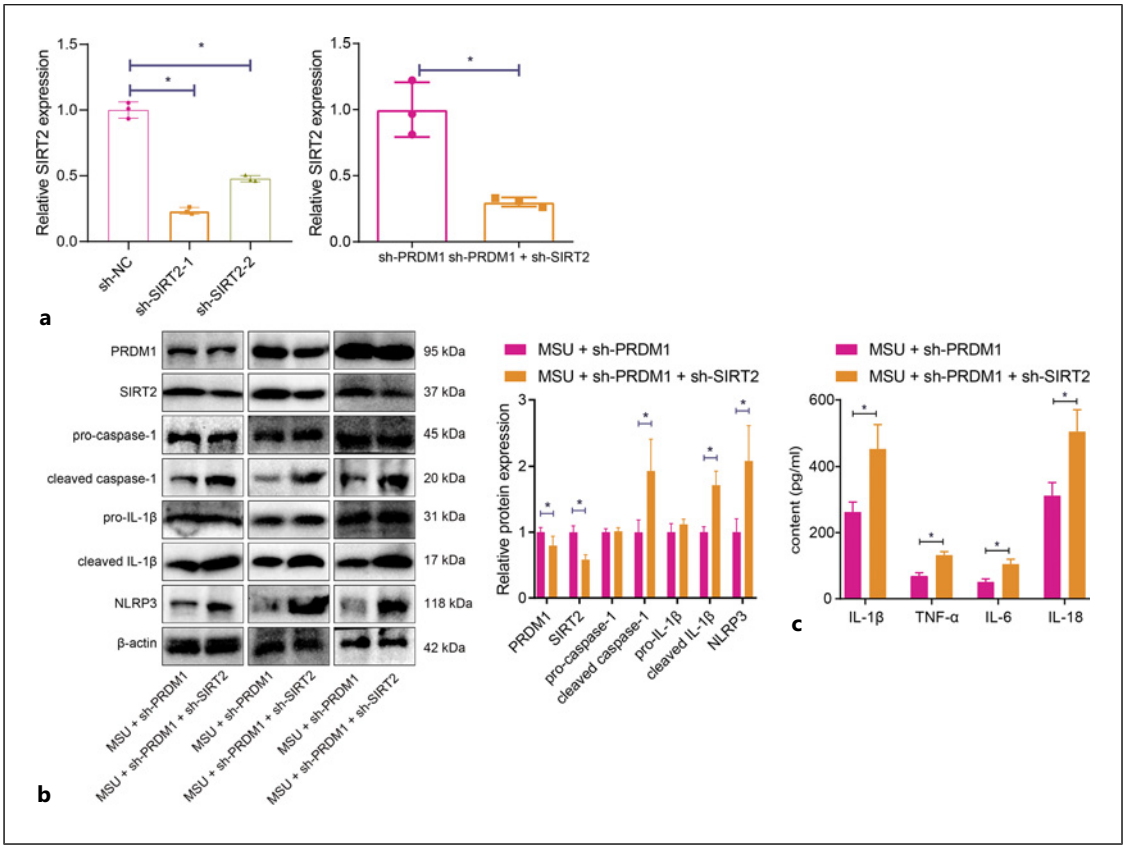

Fig. 5. PRDM1/SIRT2 axis regulates the activation of NLRP3 inflammasome and release of inflammatory cytokines from MSU-induced macrophages. **a** The silencing efficiency of sh-SIRT2-1 and sh-SIRT2-2 detected by RT-qPCR. **b** Western blot analysis of PRDM1, SIRT2, cleaved caspase-1, pro-caspase-1, cleaved IL-1β, pro-IL-1β, and NLRP3 expression in MSU-treated cells after sh-PRDM1 or sh-SIRT2 treatment normalized to MSU+ sh-NC (protein expression as 1). **c** The contents of inflammatory cytokines IL-1β, TNF-α, IL-6, and IL-18 in the supernatant of MSU-treated cell culture medium after sh-PRDM1 or sh-SIRT2 treatment. *$p < 0.05$.

verified in the context of MSU simulation, which performs a vital role in the pathogenesis of MSU-elicited acute gouty arthritis.

In the following experiments, our results found that silencing SIRT2 facilitated the accumulation of acetylated α-tubulin to increase NLRP3 inflammasome and mature IL-1β level, thus aggravating the MSU-elicited acute gouty arthritis. Importantly, an explanation to the pathogenic mechanism of acute gouty arthritis is that MSU crystals are able to induce NLRP3 inflammasome activation in monocytes or macrophages, consequently stimulating IL-1β production [22]. What's more, suppression of NLRP3 inflammasome activation can prevent acute gouty arthritis [23]. From above, we could know that NLRP3 inflammasome activation is a major cause of acute gouty arthritis. Furthermore, we found that the high level of NLRP3 inflammasome was associated with α-tubulin acetylation. Interestingly, acetylated α-tubulin is implicated in dynein-dependent mitochondrial transport and ASC binding to NLRP3 on mitochondria, and induction of α-tubulin acetylation augments the activation of NLRP3 inflammasome [18, 24]. In addition, Skoge et al. [25] reported that α-tubulin acetylation on lysine 40 was one principal way to post-translationally modify microtubules, which could be stimulated by α-tubulin N-acetyltransferase but inhibited by SIRT2. In partial accordance with our finding, knockdown of SIRT2, an NAD^+-dependent enzyme involved in the acetylation, is also conducive to triggering inflammatory responses in mice [16, 17]. Similarly, Zhang et al. claimed that assembly of NLRP3 inflammasome could be suppressed by silybin *via* regulation of the NAD^+/SIRT2 pathway [25, 26], demonstrating the potential regulatory effect of SIRT2 on the regulation of NLRP3 inflammasome. Based

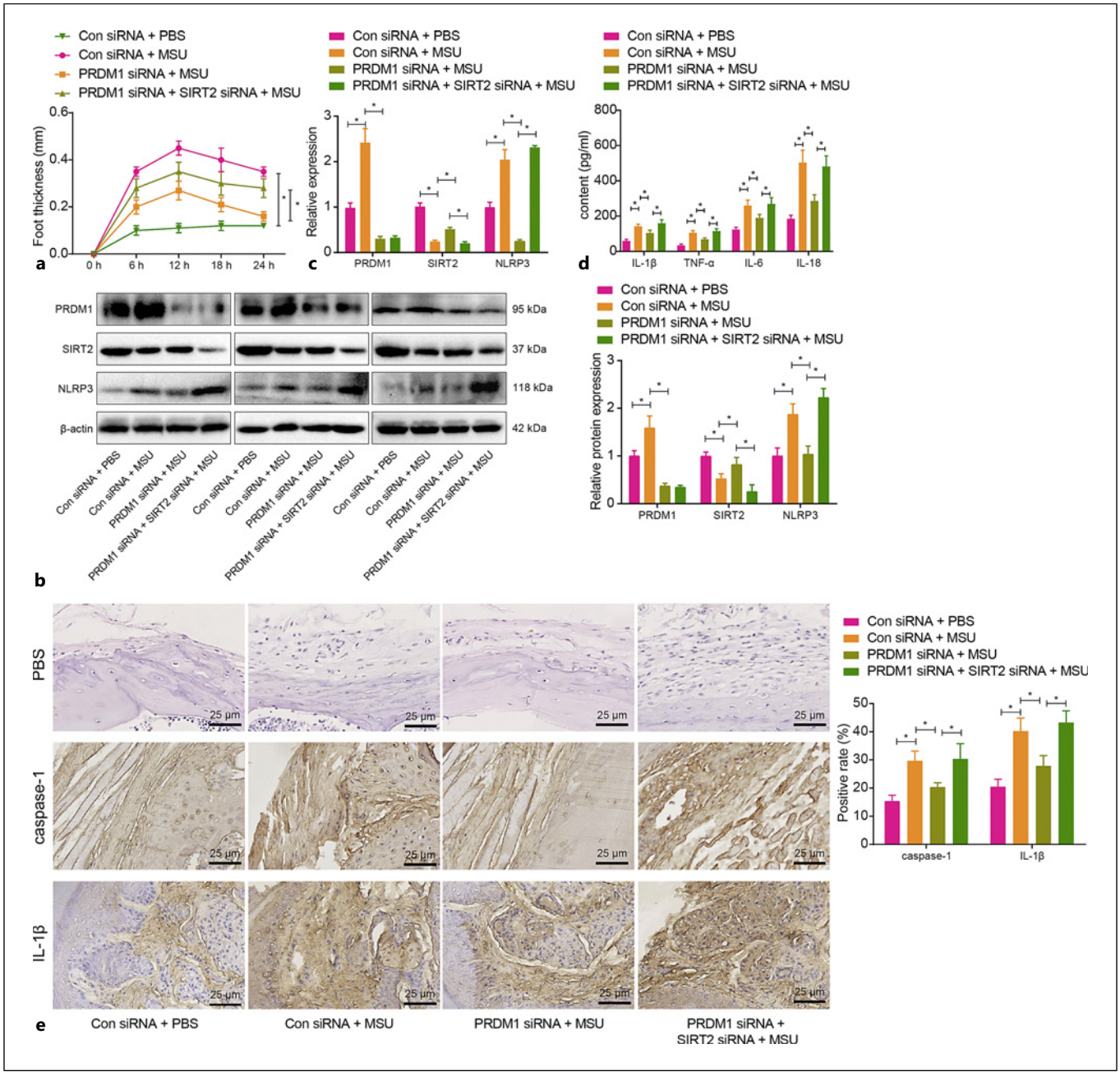

Fig. 6. The effect of PRDM1/SIRT2 axis on MSU-induced acute gouty arthritis flares is verified in vivo. **a** The thickness of mouse footpads detected at 0, 6, 12, and 24 h (n = 12). **b** The expression of PRDM1, SIRT2, and NLRP3 in mouse foot tissues detected by Western blot (n = 12). **c** The expression of PRDM1, SIRT2, and NLRP3 in mouse foot tissues detected by RT-qPCR (n = 12). **d** The levels of inflammatory cytokines IL-1β, TNF-α, IL-6, and IL-18 in the RIPA homogenous supernatant of mouse foot tissues detected by ELISA (n = 12). **e** The expression of caspase-1 and IL-1β in vectorial sections of mouse footpads detected by IHC (n = 12). *p < 0.05.

on these findings, our study further provided evidence supporting that SIRT2 negatively regulated NLRP3 inflammasome and mature IL-1β levels to deteriorate MSU-stimulated acute gouty arthritis.

Based on the experimental results, we further confirmed SIRT2 as a target gene of PRDM1. Consistently, SIRT2 is known as a class III HDAC, whilst PRDM1 response to IL21 can be restored by pan-HDAC inhibitors

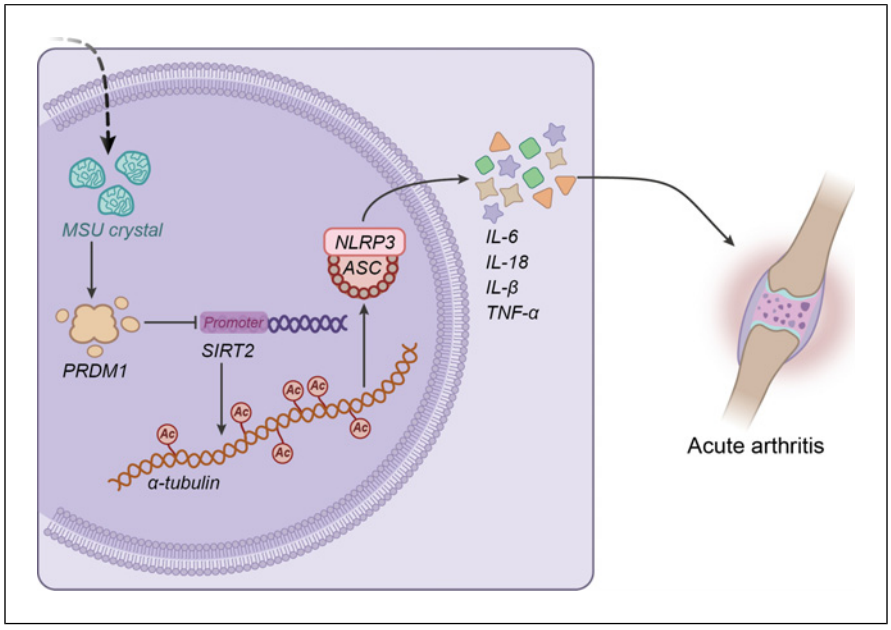

Fig. 7. The mechanism graph of the regulatory network and function of PRDM1. Increased intracellular PRDM1 expression targets the deacetylase SIRT2 to increase acetylated α-tubulin and NLRP3 inflammasome, thereby stimulating the release of the inflammatory cytokines IL-6, IL-18, IL-1β, and TNF-α from macrophages to aggravate MSU-induced acute gouty arthritis.

[27, 28]. Another previous literature has indicated that NLRP12, one NLR protein like NLRP3, acts as an important regulator for inflammatory gene expression in human myeloid cells including monocytes, and involves in the differentiation of monocytes to macrophages, while PRDM1 mediates transcriptional suppression of NLRP12 during differentiation [13]. In the present study, PRDM1 could increase the level of NLRP3 inflammasome as well as mature IL-1β level to aggravate acute gouty arthritis, which was revealed possibly to be achieved *via* downregulating SIRT2. These data partly linked PRDM1/SIRT2 to NLRP3 inflammasome activation. The above roles of PRDM1/SIRT2/NLRP3 axis were also validated in mouse models of MSU-evoked acute gouty arthritis. Altogether, we could conclude that PRDM1 contributed to the progression of MSU-stimulated acute gouty arthritis via the SIRT2/NLRP3 pathway in vitro and in vivo.

Up to now, the main findings of this study are only applicable to possible molecular mechanism involved in the regulation of acute gouty arthritis. Acute gouty arthritis, an immune system disease secondary to rheumatoid arthritis, gout, and viral infection, usually occurs at night with a short duration [1]. On the contrary, chronic gouty arthritis is defined as pain and swelling of joints that persist for more than 6 weeks, accompanied with long-term joint movement, which may lead to permanent loss of joint function [29]. The differences in disease and etiology will lead to obvious differences in treatment methods for the two contexts. What we are exploring is the possible molecular mechanism of acute gouty arthritis, while the specific molecular mechanism behind chronic gouty arthritis still needs new exploration. Acute gouty arthritis can be treated with nondrug therapy such as ice pack for pain relieving and some anti-inflammatory drugs, while chronic gouty arthritis requires long-term treatment for reduction of serum uric acid [30]. Colchicine is an alkaloid extract from plants of the genus Colchicum (autumn crocus), and its therapeutic use has been demonstrated in gout [1, 31]. The primary action mechanism of colchicine is tubulin disruption, which results in subsequent blockade of multiple inflammatory pathways and regulation of innate immunity [32]. There are several newly reported mechanisms including diverse inhibitory effects on macrophages such as repression of NALP3 inflammasome, suppression of pore formation activated by purinergic receptors P2X7 and P2X2, and promotion of dendritic cell maturation and antigen presentation [33, 34]. Therefore, whether colchicine will affect the regulatory pathways found in this study deserves further discussion.

To sum up, this paper proposed that MSU crystals increased PRDM1 expression in macrophages, and PRDM1 decreased the expression of the deacetylase SIRT2, thereby causing deposition of acetylated α-tubulin and increasing the level of NLRP3 inflammasome. In this context, macrophages will release large amounts of inflammation-promoting IL-6, IL-18, IL-1β, and TNF-α, ultimately inducing the progression of MSU-induced acute gouty arthritis. This is a new molecular mechanism involved in the pathogenesis of acute gouty arthritis,

which may provide new biomarkers or targets for treating this disease. However, PRDM1 knockdown and the dual knockdown of PRDM1 and SIRT1 would be performed in the future to further support the claim in animal models.

Statement of Ethics

All research protocols were approved by the Clinical Research Ethics Committee and Animal Ethics Committee of the Fourth Affiliated Hospital of Harbin Medical University (2016-393-2) and in keeping with the Declaration of Helsinki for human beings and NIH guidelines for animals. Written informed consent to participate in this study was obtained from patients and for the participants aged under 18, written informed consent to participate in this study was obtained from their legal guardians.

Conflict of Interest Statement

The authors declare that they have no conflict of interest.

Funding Sources

This study was supported by Applied Technology Research and Development Fund of Harbin Science and Technology Bureau in 2017 (Innovative Talent Project) (2017RAXXJ067), The Fourth Affiliated Hospital of Harbin Medical University Dean Fund (HYDSYYZ201502), Natural Science Foundation of Heilongjiang Province (LH2020H063), Outstanding Youth Fund of the Fourth Hospital of Harbin Medical University (HYDSYYXQN202008), Heilongjiang Provincial Academy of Science and Technology Cooperation Project (YS18C06); Heilongjiang Province Postdoctoral Fund (LBH-Z21170), Sichuan Provincial Western Psychiatric Association's CSPC LEADING Scientific Research Project and Study on the mechanism of GDF10 to promote the vascular regeneration and travel of diabetic foot microartery.

Author Contributions

Qingsong Zhao, Nan Xia, Jinmei Xu, and Yingnan Wang designed the study. Zhifeng Cheng collected the data, designed and developed the database, carried out data analyses, and produced the initial draft of the manuscript. Luwen Feng, Dihan Su, and Qingsong Zhao contributed to drafting the manuscript. All authors have read and approved the final submitted manuscript.

Data Availability Statement

All data generated or analyzed during this study are included in this article and its online supplementary material. Further inquiries can be directed to the corresponding author.

References

1 Wilson L, Saseen JJ. Gouty arthritis: a review of acute management and prevention. Pharmacotherapy. 2016;36(8):906–22.
2 Punzi L, Scanu A, Galozzi P, Luisetto R, Spinella P, Scire CA, et al. One year in review 2020: gout. Clin Exp Rheumatol. 2020;38(5):807–21.
3 Liu L, Zhu L, Liu M, Zhao L, Yu Y, Xue Y, et al. Recent insights into the role of macrophages in acute gout. Front Immunol. 2022;13:955806.
4 Li X, Gao J, Tao J. Purinergic signaling in the regulation of gout flare and resolution. Front Immunol. 2021;12:785425.
5 Desai J, Steiger S, Anders HJ. Molecular pathophysiology of gout. Trends Mol Med. 2017;23(8):756–68.
6 So AK, Martinon F. Inflammation in gout: mechanisms and therapeutic targets. Nat Rev Rheumatol. 2017;13(11):639–47.
7 Tran TH, Pham JT, Shafeeq H, Manigault KR, Arya V. Role of interleukin-1 inhibitors in the management of gout. Pharmacotherapy. 2013;33(7):744–53.
8 Schlesinger N. Anti-interleukin-1 therapy in the management of gout. Curr Rheumatol Rep. 2014;16(2):398.
9 Lee K, Jang SH, Tian H, Kim SJ. NonO is a novel Co-factor of PRDM1 and regulates inflammatory response in monocyte derived-dendritic cells. Front Immunol. 2020;11:1436.
10 Kim GD, Das R, Goduni L, McClellan S, Hazlett LD, Mahabeleshwar GH. Kruppel-like factor 6 promotes macrophage-mediated inflammation by suppressing B cell leukemia/lymphoma 6 expression. J Biol Chem. 2016;291(40):21271–82.
11 Ulmert I, Henriques-Oliveira L, Pereira CF, Lahl K. Mononuclear phagocyte regulation by the transcription factor Blimp-1 in health and disease. Immunology. 2020;161(4):303–13.
12 Mylona EE, Mouktaroudi M, Crisan TO, Makri S, Pistiki A, Georgitsi M, et al. Enhanced interleukin-1β production of PBMCs from patients with gout after stimulation with Toll-like receptor-2 ligands and urate crystals. Arthritis Res Ther. 2012;14(4):R158.
13 Lord CA, Savitsky D, Sitcheran R, Calame K, Wright JR, Ting JP, et al. Blimp-1/PRDM1 mediates transcriptional suppression of the NLR gene NLRP12/Monarch-1. J Immunol. 2009;182(5):2948–58.
14 Martinon F, Petrilli V, Mayor A, Tardivel A, Tschopp J. Gout-associated uric acid crystals activate the NALP3 inflammasome. Nature. 2006;440(7081):237–41.
15 Karasawa T, Takahashi M. The crystal-induced activation of NLRP3 inflammasomes in atherosclerosis. Inflamm Regen. 2017;37:18.
16 Mendes KL, Lelis DF, Santos SHS. Nuclear sirtuins and inflammatory signaling pathways. Cytokine Growth Factor Rev. 2017;38:98–105.
17 North BJ, Marshall BL, Borra MT, Denu JM, Verdin E. The human Sir2 ortholog, SIRT2, is an NAD+-dependent tubulin deacetylase. Mol Cell. 2003;11(2):437–44.
18 Misawa T, Takahama M, Kozaki T, Lee H, Zou J, Saitoh T, et al. Microtubule-driven spatial arrangement of mitochondria promotes activation of the NLRP3 inflammasome. Nat Immunol. 2013;14(5):454–60.
19 Neogi T, Jansen TL, Dalbeth N, Fransen J, Schumacher HR, Berendsen D, et al. 2015 gout classification criteria: an American College of Rheumatology/European league against rheumatism collaborative initiative. Ann Rheum Dis. 2015;74(10):1789–98.

20 Liu L, Xue Y, Zhu Y, Xuan D, Yang X, Liang M, et al. Interleukin 37 limits monosodium urate crystal-induced innate immune responses in human and murine models of gout. Arthritis Res Ther. 2016;18(1):268.
21 Wu M, Tian Y, Wang Q, Guo C. Gout: a disease involved with complicated immunoinflammatory responses – a narrative review. Clin Rheumatol. 2020;39(10):2849–59.
22 Chung YH, Kim HY, Yoon BR, Kang YJ, Lee WW. Suppression of Syk activation by resveratrol inhibits MSU crystal-induced inflammation in human monocytes. J Mol Med. 2019;97(3):369–83.
23 Lee HE, Yang G, Park YB, Kang HC, Cho YY, Lee HS, et al. Epigallocatechin-3-Gallate prevents acute gout by suppressing NLRP3 inflammasome activation and mitochondrial DNA Synthesis. Molecules. 2019;24(11):2138.
24 Li CG, Zeng QZ, Chen MY, Xu LH, Zhang CC, Mai FY, et al. Evodiamine augments NLRP3 inflammasome activation and anti-bacterial responses through inducing α-tubulin acetylation. Front Pharmacol. 2019;10:290.
25 Skoge RH, Dolle C, Ziegler M. Regulation of SIRT2-dependent α-tubulin deacetylation by cellular NAD levels. DNA Repair. 2014;23:33–8.
26 Zhang B, Xu D, She L, Wang Z, Yang N, Sun R, et al. Silybin inhibits NLRP3 inflammasome assembly through the NAD(+)/SIRT2 pathway in mice with nonalcoholic fatty liver disease. FASEB J. 2018;32(2):757–67.
27 He FF, You RY, Ye C, Lei CT, Tang H, Su H, et al. Inhibition of SIRT2 alleviates fibroblast activation and renal tubulointerstitial fibrosis via MDM2. Cell Physiol Biochem. 2018;46(2):451–60.
28 Desmots F, Roussel M, Pangault C, Llamas-Gutierrez F, Pastoret C, Guiheneuf E, et al. Pan-HDAC inhibitors restore PRDM1 response to IL21 in CREBBP-mutated follicular lymphoma. Clin Cancer Res. 2019;25(2):735–46.
29 Schlesinger N, Lipsky PE. Pegloticase treatment of chronic refractory gout: update on efficacy and safety. Semin Arthritis Rheum. 2020;50(3S):S31–8.
30 Schlesinger N. Management of acute and chronic gouty arthritis: present state-of-the-art. Drugs. 2004;64(21):2399–416.
31 Leung YY, Yao Hui LL, Kraus VB. Colchicine: update on mechanisms of action and therapeutic uses. Semin Arthritis Rheum. 2015;45(3):341–50.
32 Bhattacharyya B, Panda D, Gupta S, Banerjee M. Anti-mitotic activity of colchicine and the structural basis for its interaction with tubulin. Med Res Rev. 2008;28(1):155–83.
33 Nuki G. Colchicine: its mechanism of action and efficacy in crystal-induced inflammation. Curr Rheumatol Rep. 2008;10(3):218–27.
34 Dalbeth N, Lauterio TJ, Wolfe HR. Mechanism of action of colchicine in the treatment of gout. Clin Ther. 2014;36(10):1465–79.